Bifurcation and Chaos in a Simple Passive Bipedal Gait

Benoit Thuilot Ambarish Goswami Bernard Espiau

INRIA Rhône-Alpes
655 avenue de l'Europe, ZIRST
38330 Montbonnot Saint Martin, France
Benoit.Thuilot@inrialpes.fr

Abstract

This paper proposes an analysis of the behavior of perhaps the simplest biped robot: the compass gait model. It has been shown previously that such a robot can walk down a slope indefinitely without any actuation. Passive motions of this nature are of particular interest since they may lead us to strategies for controlling active walking machines as well as to a better understanding of human locomotion. We show here that, depending on the parameters of the system, passive compass gait may exhibit 1-periodic, 2^n-periodic and chaotic gaits proceeding from cascades of period-doubling bifurcations. Since compass equations are quite involved (they combine nonlinear differential and algebraic equations in a 4-dimensional space), our investigations rely, in part, on numerical simulations.

1 Motivation

At the INRIA Rhône-Alpes Laboratory of Grenoble, France, we are working on the development of an anthropomorphic biped walker. The envisioned prototype will have reasonable adaptation capability on an unforeseen uneven terrain. The purpose of the project is not limited to the realization of a complex machine, the construction and control of which nevertheless pose formidable engineering challenge. We also intend to initiate a synergy between robotics and human gait study. Human locomotion, despite being well studied and enjoying a rich database, is not well understood and a robotic simulcrum potentially can be very useful.

In order to gain a better understanding of the inherently nonlinear dynamics of a full-fledged walking machine we have found it instructive to first explore the behavior of a particularly simple, perhaps the simplest, walker model. Based on the same kinematics as that of a double pendulum, the Acrobot [1] and the Pendubot [4] are the nearest cousins of the compass gait model studied here. While decomposing human locomotion into sub-motions, compass gait appears at the most elementary level, [18] [21]. It has therefore received abundant attention from biped robot community. One of the earliest works on compass gait may be tracked to [12] and [5]. It has been subsequently discussed in [17], using a linearizing approach. In order to get a better understanding of the compass behavior, nonlinear methods are now employed, [8]. We follow here an approach parallel to that developed in [8], but we do not add the simplifying assumptions to the compass model.

We focus here on passive (or unactuated) compass gaits along an inclined plane. A passive motion has a special appeal because it is *natural* and it does not require any external energy source. If an active control law closely mimics a passive system it is likely to enjoy certain inherent advantages of the passive system such as the energy optimality, periodicity, and stability. Of particular interest in this respect is the hypothesis that a great part of the swing stage in human locomotion is passive, a hypothesis that is supported by many studies ([18] for instance).

Despite the fact that the compass has a simple kinematics, its analysis is complicated since its governing equations are of hybrid nature consisting of nonlinear ODEs and algebraic switching conditions. Moreover, since the system state-space is 4-dimensional, we cannot take advantage of the visual depiction of the state trajectories. We therefore turn towards systematic numerical simulations. Depending on the length and mass parameters of the model, the compass undergoes period-doubling bifurcations leading eventually to chaotic motion. Discussion of this behavior is the object of this paper. The results obtained are parallel to those established for the planar monopod which has a different dynamics and a lower dimensional state-space [24], [19], [7].

The paper is organized as follows: compass model is described in Section 2. A typical gait pattern is then briefly discussed in Section 3. The limit of the linearizing approach is identified in Section 4. Section 5 is devoted to a systematic numerical analysis of the compass gait, with a special emphasis on complex gaits (asymmetric and chaotic gaits). Section 6 presents finally the future lines of research that we intend to pursue.

2 Governing equation, normalization

2.1 Model description

The biped robot considered here, hereafter called *compass*, consists of two identical legs jointed at the hip, see Fig. 1. The mass is concentrated at 3 points: at the hip, m_H, and on each leg, m, at distances a and b respectively from the leg tip and the hip. For forthcoming simulation trials, the mass ratio $\mu = \frac{m_H}{m}$ and the length ratio $\beta = \frac{b}{a}$ will be varied from 0.1 to 10 when total mass $m_C = 2m + m_H$ and leg length $l = a+b$ are constant and equal, respectively, to 20 Kg and 1 meter. This compass walks down on a plane surface possessing a constant slope ϕ.

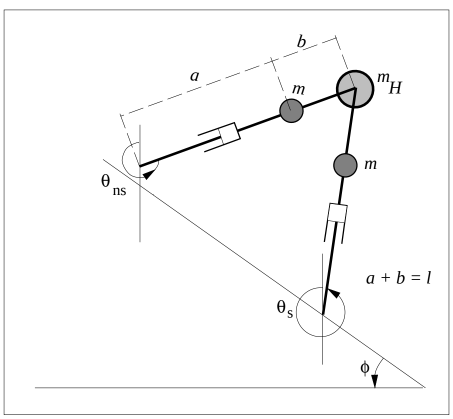

Figure 1: Model of a compass-like biped robot

The compass gait consists of two stages:

- *Swing:* the compass hip pivots around the point of support of its *support leg* on the ground. The other leg, called the *non-support leg* or the *swing leg* swings forward. The tip of the support leg is assumed slipless. The compass is kinematically equivalent to a double-pendulum.

  The configuration of the compass can be described by $\boldsymbol{\theta} = [\theta_{ns}, \theta_s]^T$ with θ_{ns} and θ_s the angles made respectively by the non-support and the support leg with the vertical (counterclockwise positive). The compass state vector is then $\boldsymbol{q} = [\boldsymbol{\theta}, \dot{\boldsymbol{\theta}}]^T$.

- *Transition:* the support is transferred, instantaneously, from one leg to the other. The impact of the swing leg with the ground is assumed to be inelastic and without sliding. The half-inter leg angle α will be used to characterize transition.

A knee-less compass with a rigid leg cannot however clear the ground. This conceptual problem is avoided by including below point mass m a prismatic-jointed knee with a telescopically retractable massless lower leg, see Fig. 1. This obviously solves the problem of foot clearance without affecting compass dynamics.

The simplifying assumptions described here are not unique to this work, they are routinely made in the biped robot literature and compass prototypes have also been actually developed, see [17], [11].

2.2 The governing equations

The computational details regarding the derivation of the compass equations and the proofs of the normalization properties can be found in [14].

Swing stage The dynamic equations of the swing stage are similar to the well-known double-pendulum equations. Since the legs of the compass are assumed identical, the equations are similar regardless of the support leg considered. They have the following form:

$$\dot{\boldsymbol{q}} = \begin{pmatrix} \dot{\boldsymbol{\theta}} \\ -\boldsymbol{M}^{-1}(\boldsymbol{\theta}) \left[\boldsymbol{N}(\boldsymbol{\theta}, \dot{\boldsymbol{\theta}})\dot{\boldsymbol{\theta}} + \frac{1}{a}\boldsymbol{g}(\boldsymbol{\theta}) \right] \end{pmatrix} \quad (1)$$

where $\boldsymbol{M}(\boldsymbol{\theta})$ is the 2×2 inertia matrix, symmetric positive definite, $\boldsymbol{N}(\boldsymbol{\theta}, \dot{\boldsymbol{\theta}})$ is a 2×2 matrix with the centrifugal terms, and $\frac{1}{a}\boldsymbol{g}(\boldsymbol{\theta})$ is a 2×1 vector of gravitational torques. Eqs. (1) are normalized with respect to mass and length parameters: $\boldsymbol{M}(\boldsymbol{\theta})$, $\boldsymbol{N}(\boldsymbol{\theta}, \dot{\boldsymbol{\theta}})$ and $\boldsymbol{g}(\boldsymbol{\theta})$ depend not on m, m_H, a and b, but only on μ and β.

Transition stage According to our collision assumptions (inelastic and non-sliding), the compass configuration is unchanged during the instantaneous transition, but leg angular velocity undergoes a discontinuous jump, [15], [8]. Transition equations can be shown to be of the form:

$$\boldsymbol{q}^+ = \boldsymbol{W}(\alpha)\boldsymbol{q}^- \quad (2)$$

with:

$$\boldsymbol{W}(\alpha) = \begin{pmatrix} \boldsymbol{J} & 0 \\ 0 & \boldsymbol{H}(\alpha) \end{pmatrix}$$

The superscripts $^-$ and $^+$ identify respectively pre-impact and post-impact quantities. The matrix $\boldsymbol{J}$:

$$\boldsymbol{J} = \begin{pmatrix} 0 & 1 \\ 1 & 0 \end{pmatrix}$$

exchanges the support and the swing leg angles for the upcoming swing stage. The matrix $\boldsymbol{H}(\alpha)$ follows from the conservation, during impact, of compass angular momentum about the point of impact. The matrix $\boldsymbol{W}(\alpha)$ also depends only on the dimensionless ratios μ and β.

Parameters of interest Since all matrices in Eqs. (1) and (2) are normalized with respect to mass and length parameters, it follows that ([14]) :

Gait characteristics of a compass with arbitrary masses m and m_H (resp. lengths a and b) can always be deduced from those of a compass whose masses (resp. lengths) are in the same proportion μ (resp. β).

A comprehensive analysis of compass gait characteristics with respect to its structural parameters can therefore be achieved by considering solely the variations of μ and β and those of slope ϕ.

3 A typical limit cycle

Simulation trials reveal that for a certain set of initial conditions, a passive compass presents a steady gait, i.e., can walk down a slope indefinitely without falling down. This steady gait corresponds to a *stable limit cycle* of the compass equations (1) and (2), and the set of initial conditions converging towards it is its *basin of attraction*. As a first insight, we discuss here a *symmetric* or *1-periodic gait* using a phase portrait. Since we cannot graphically visualize the full 4D phase space, we limit ourselves to a 2D projection of the compass' phase portrait consisting of the displacement vs. the velocity of only one leg, the leg shown in dotted in Fig. 2. The upper half of the cycle (I→II) corresponds to the swing stage of the dotted leg, and the lower half (III→IV) corresponds to its support stage (indicated by a black dot on the stick diagram of Fig. 2). The 2 vertical lines (II→III) and (IV→I) correspond to the velocity jumps during instantaneous transition.

Such a permanent regime passive gait is conceivable since the precise amount of kinetic energy gain due to the conversion of gravitational potential energy during a step is absorbed in the instantaneous impact at the touchdown. The mechanical energy of the compass is therefore constant during the all walk[1].

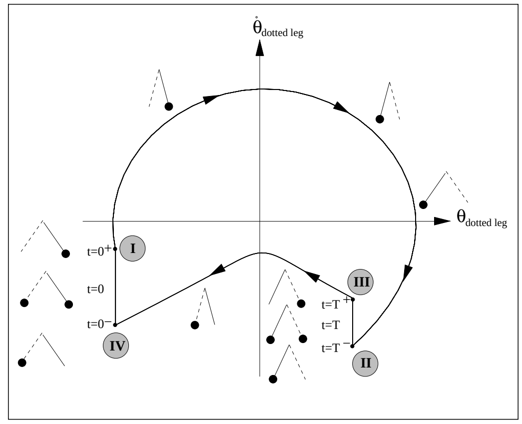

Figure 2: Phase portrait of a steady gait

4 Limitations of the linearized model

To our knowledge, there is no analytical method of studying the limit cycles of hybrid systems such as the compass. One approach is to linearize the swing stage equations around the equilibrium $\boldsymbol{q} = \boldsymbol{0}$, in such a way that the dynamic evolution of the compass can be computed analytically. All compass gait characteristics can then be determined explicitly, in particular $\boldsymbol{q}_l^*$, the state vector of the linearized compass when it describes the limit cycle. Our hope is that $\boldsymbol{q}_l^*$ at least belongs to the basin of attraction of the actual compass limit cycle, so that the robot converges to it after the transients have died down.

For a given compass, this approach has been shown to be successful for slopes less than 1.4°, [17]. The simulations described below have shown that linearization is actually successful for small ϕ and small β. Specifically, starting from $\boldsymbol{q}_l^*$, the actual compass with any $\mu \in [0.1, 10]$ converges to a steady gait:

for $\beta < 4.8$ when $\phi = 0.25°$, for $\beta < 1.5$ when $\phi = 3°$,
for $\beta < 2.9$ when $\phi = 1.5°$, for $\beta < 1$ when $\phi = 4°$.

5 Behavior of the nonlinear model

Compass equations (1)-(2) have been simulated using *SCILAB-2.2* [22]. The 3 compass parameters ϕ, μ and β identified in Section 2.2 were varied in a systematic way, and 3 gait variables, the step-period T, the half inter-leg angle at touchdown α and the total mechanical energy E of the compass were observed. For small ϕ, μ and β, the gait is symmetric, as described

[1]Note that this is the "local" mechanical energy. Since the compass physically continues to descend down the slope, its potential energy keeps decreasing.

in Section 5.1. For higher values of the parameters, the robot exhibits period-doubling phenomena, as described in Section 5.2.

5.1 Symmetric gaits

It is interesting to note that for a given triplet (ϕ, μ, β), we have never identified more than one steady gait. Moreover, when the gait remains symmetric, all of the gait variables evolve monotonically. This reinforces our suspicion that, for a given compass with parameters μ and β, the ground slope ϕ *uniquely* defines all gait variables. Since this is not an analytical result, we cannot claim it as a proof. The property of monotonic evolution of the variables is nevertheless exploited in [6], [9] and [10] in formulating control strategies for the compass. It is shown that a scalar control law which seeks to converge the mechanical energy of the "actively controlled" compass to that corresponding to a known passive gait ensures, in fact, the convergence of *all* the state variables of the compass.

Figs. 3 (a-c), 4 (a-c) and 5 (a-c) present the evolution of the variables T, α and E as functions, respectively, of the parameters ϕ, μ and β. They are known as *bifurcation diagrams* [3][13][16]. Period-doubling phenomena, which give rise to several branches[2] will be discussed in the following section. The chaotic gait, represented by a continuous distribution of points in Figures 3(a) and 3(b), is omitted for the sake of clarity in all subsequent bifurcation diagrams. Finally, Figs. 3 (d), 4 (d) and 5 (d) present several phase plane diagrams.

These numerical simulations show that the compass takes longer and faster steps when ϕ or μ are increased and longer but slower steps when β is increased. This behavior can also be summarized as follows:

	T	L	E	v
when $\phi \nearrow$	$\nearrow$	$\nearrow$	$\nearrow$	$\nearrow$
when $\mu \nearrow$	$\nearrow$	$\nearrow$	$\nearrow$	$\nearrow$
when $\beta \nearrow$	$\nearrow$	$\nearrow$	$\searrow$	$\searrow$

where L and v denote respectively the step length, i.e. $L = 2l \sin\alpha$, (cf. Fig. 1) and the average velocity, i.e. $v = \frac{L}{T}$.

The evolution of v can be made more precise using Figs. 3 (d), 4 (d) and 5 (d): when ϕ is increased, phase plane diagrams are enlarged in both directions. Therefore v clearly increases. When μ and β are increased, phase plane diagrams are compressed in the $\dot{\theta}$-direction, but enlarged in the θ-direction. We deduce immediately that the maximum angular velocity decreases when μ and β are increased. Plotting $v = \frac{L}{T}$ shows that the average velocity nevertheless grows when μ is increased. On the contrary v decreases when β is increased. In addition, for small β, i.e. the mass center of the leg is near the hip, the angular velocity of the support leg is almost constant during the swing.

Results regarding E can be interpreted as follows: when ϕ is increased, the potential energy P varies just a tiny bit. The kinetic energy K, however, increases since v grows. Therefore E has to grow when ϕ is increased. When μ *(resp. β)* is increased, compass center of mass rises *(resp. lowers)*, and so does P. The change in K is negligible compared to that in P. Therefore E has to increase *(resp. decrease)* when μ *(resp. β)* is increased.

5.2 Bifurcations and chaotic gait

For higher values of all of the parameters ϕ, μ and β, the compass exhibits *period-doubling* phenomena [3], [13], [16], also termed *flip bifurcations* [23]. In this case, the compass gait, previously symmetric, is modified to a series of asymmetric 2^n-periodic gaits with progressively higher values of n. For sufficiently higher values of the parameters the gait becomes chaotic.

This behavior can be explained as follows: let $\boldsymbol{q}_k$ be the compass state vector at the beginning of the k^{th} step. The first return map of Poincaré of the compass depends on all the three parameters mentioned above. It will be written as $\boldsymbol{q}_{k+1} = F_{\phi,\mu,\beta}(\boldsymbol{q}_k)$. When the compass gait is symmetric, $F_{\phi,\mu,\beta}$ possesses a stable fixed point $\boldsymbol{q}^*$, i.e. $\boldsymbol{q}^* = F_{\phi,\mu,\beta}(\boldsymbol{q}^*)$.

If we continuously modify the parameters, the mapping $F_{\phi,\mu,\beta}$ is also modified, and the fixed point is at first shifted, but for a given value of the parameters, it may turn unstable. In the case of the compass, the *structural unstability* of the fixed point results in a period-doubling, i.e. there is the sudden appearance of two points $\boldsymbol{q}^*$ and $\bar{\boldsymbol{q}}^*$ which are inter-related as:

$$\bar{\boldsymbol{q}}^* = F_{\phi,\mu,\beta}(\boldsymbol{q}^*) \quad \text{and} \quad \boldsymbol{q}^* = F_{\phi,\mu,\beta}(\bar{\boldsymbol{q}}^*)$$

The passive walk of the compass is then the indefinite repetition of the two different gaits $\boldsymbol{q}^*$ and $\bar{\boldsymbol{q}}^*$. Each of these gaits undergoes period-doublings for higher values of the parameters, giving rise to 2^n-periodic gaits.

A cascade of period-doublings, associated with an increase of ϕ when $\mu = 2$ and $\beta = 1$, is depicted in Fig. 6: the k^{th} vs. $k{+}1^{th}$ touchdown angular positions

[2] whose arithmetic average is represented by the dotted line.

of the non-support leg when the compass takes its passive gait are plotted. For a symmetric gait the touchdown angular position is the same in every cycle. It is then represented by a point on the line $\theta(k) = \theta(k+1)$. As we change the ground slope, the touchdown position gradually shifts along this line. For $\phi = 4.37°$, the compass gait becomes 2-periodic, giving rise in Fig. 6 to 2 points moving away from the $\theta(k) = \theta(k+1)$ line along the two branches shown by dotted lines. One step length is slightly longer and the other slightly shorter than the corresponding symmetric gait. Subsequent bifurcations occur at $\phi = 4.9°$ and $\phi = 5.01°$, giving rise respectively to a 4-periodic and a 8-periodic gait. These gaits are nevertheless strictly ordered: the compass takes these 4 or 8 steps always in the same order, and a long step is always followed by a short one. The bifurcation behavior of the compass may also be observed in the phase space limit cycle as well. Fig. 7 presents the cycles corresponding to a 4-periodic gait.

The first bifurcations are easy to detect since the range of variation of the parameters from one bifurcation to the next are relatively large. The subsequent bifurcations occur for relatively smaller changes in the parameter values and are often difficult to segregate individually. This is a general property of any system which undergoes a cascade of period-doublings. In the case of the compass, at $\phi = 5.03°$, the passive gait is 8-periodic. During the interval of $\phi = 5.03° \rightarrow 5.04°$ a cascade of period-doublings takes place and at $\phi = 5.04°$ we are unable to detect any periodicity in the motion of the compass. However, an order is still maintained in this gait – a long step is always followed by a short one. This indicates that the gait is not chaotic but is a 2^n-periodic gait with n large.

For $\phi = 5.2°$, the compass gait can be said to be truly chaotic. A chaotic gait is qualitatively characterized by the presence of a "broad-band frequency" as we find in Figure 8(a) in our histogram of the step periods. Following [8], this property can also be exhibited by plotting the first return map of the touchdown angular position of the compass leg, as shown in Fig. 8(b). Finally Figure 8(c) shows the phase trajectories of the compass: they stay on a strange attractor which is a manifold of a lower dimension in the phase space. We have computed its fractal dimension to be equal to 2.06.

Such period-doubling cascades leading to chaotic behavior have already been observed for passive hopping robots: 2^n-periodic gaits were observed in [20] (they were termed "limping gaits"), and analyzed in [24], [19] [2] and [7].

6 Conclusions and Future Work

We have studied the stability and the periodicity properties of the passive motion of a simple biped machine termed as compass gait. There is a strong indication that all the motion descriptors for a compass with given parameters (μ, β) is completely specified by the slope of the inclined plane. The motion equations exhibit a cascade of flip bifurcations leading to a chaotic gait when the slope is increased or the compass mass or geometric parameters are modified.

Although not useful as a viable "walk", the *unstable* limit cycles exhibited by the compass may tell us more about its global properties. To identify them, we would need to integrate the system back in time.

We should also remember that our system's behavior is influenced by our impact model which is not, by any means, the only available impact model. For the impact model to be of practical use the compass gait should be robust against small parameter perturbations in the model. In order to quantify this point, it would be useful to be able to identify the boundary of the basin of attraction.

Finally it is instructive to remember that the difficulty in studying the behavior of this apparently simple biped mechanism is to a large part due to its *hybrid* differential-algebraic governing equations which makes it especially difficult for us to employ the traditional nonlinear systems tools in our current study.

References

[1] M.D. Berkemeier and R.S. Fearing. Control of a two-link robot to achieve sliding and hopping gaits. In *Proc. of IEEE Conf. on Robotics and Automation*, volume 1, pages 286–291, Nice, 1992.

[2] M. Buehler and D.E. Koditschek. Analysis of a simplified hopping robot. *International Journal of Robotics Research* 10(6): 587-605, 1991.

[3] P. Bergé, Y. Pomeau, and C. Vidal. *Order within chaos*. John Wiley & sons, 1984.

[4] D.J. Block and M.W. Spong. Mechanical design & control of the pendubot. In *SAE Earthmoving Industry Conference*, Peoria, IL, 1995.

[5] B. Bavarian, B.F. Wyman, and H. Hemami. Control of the constrained planar simple inverted pendulum. *Int. J. of Control*, 37(4):344–358, 1983.

[6] B. Espiau and A. Goswami. Compass gait revisited. In *Proc. IFAC Symposium on Robot Control (SYROCO)*, pages 839–846, Capri, Septembre 1994.

[7] C. François. *Contribution à la locomotion articulée dynamiquement stable (in French)*. PhD thesis, Ecole des Mines de Paris, April 1996.

[8] M. Garcia, A. Chatterjee, M. Coleman, and A. Ruina. Complex behavior of the simplest walking model. submitted to Journal of Biomechanics, 1996.

[9] A. Goswami, B. Espiau, and A. Keramane. Limit cycle and their stability in a passive bipedal gait. In *Proc. of IEEE Int. Conf. on Robotics and Automation*, pages 246–251, Minneapolis, April 1996.

[10] A. Goswami, B. Espiau, and A. Keramane. Limit cycles in a passive compass gait biped and passivity-mimicking control laws. accepted for *Journal of Autonomous Robots*, 1997.

[11] A.A. Grishin, A.M. Formalsky, A.V. Lensky, and S.V. Zhitomirsky. Dynamic walking of a vehicule with two telescopic legs controlled by two drives. *The International Journal of Robotics Research*, 13(2):137–147, April 1994.

[12] C. L. Golliday and H. Hemami. An approach to analyzing biped locomotion dynamics and designing robot locomotion controls. *IEEE Trans. on Aut. Cont.*, 22(6):963–972, 1977.

[13] J. Guckenheimer and P. Holmes. *Nonlinear Oscillations, Dynamical Systems, and Bifurcations.* Springer-Verlag, New York, 1983.

[14] A. Goswami, B. Thuilot, and B. Espiau. Compass-like biped robot, Part I: stability and bifurcation of passive gaits. Research Report n° 2996, INRIA, October 1996.

[15] Y. Hurmuzlu and T.H. Chang. Rigid body collisions of a special class of planar kinematic chains. *IEEE Transactions on Systems, Man and Cybernetics*, 22(5):964–971, 1992.

[16] R. C. Hilborn. *Chaos & Nonlinear Dynamics.* Oxford University Press Inc., 1994.

[17] T. McGeer. Passive dynamic walking. *Int. J. of Rob. Res.*, 9(2):62–82, 1990.

[18] T.A. McMahon. *Muscles, Reflexes, and Locomotion.* Princeton University Press, 1984.

[19] J.P. Ostrowski and J.W. Burdick. Designing feedback algorithms for controlling the periodic motions of legged robots. In *Proc. IEEE Int. Conf. on Robotics & Automation*, volume 2, pages 260–266, Atlanta, May 1993.

[20] M.H. Raibert. *Legged Robots that Balance.* MIT Press, Cambridge, USA, 1986.

[21] J. Rose and J.G. Gamble (eds). *Human Walking.* Williams & Wilkins, Baltimore, USA, 1994.

[22] *Scilab-2.2.* INRIA Rocquencourt, France. February 1996.

[23] H. Troger and A. Steindl. *Nonlinear stability and bifurcation theory.* Springer Verlag, Wien, 1991.

[24] A.F. Vakakis and J.W. Burdick. Chaotic motions in the dynamics of a hopping robot. In *Proc. IEEE Int. Conf. on Robotics & Automation*, pages 1464–1469, Cincinnati, 1990.

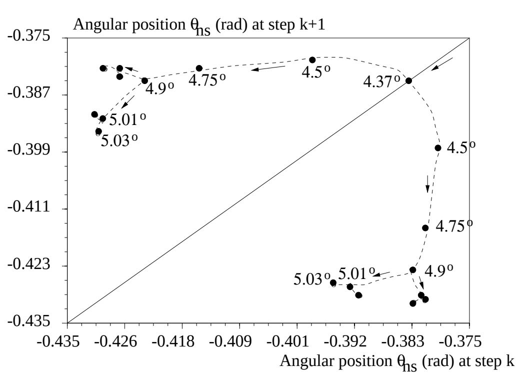

Figure 6: First return map of θ_{ns}: 2^n-periodic gait, $n \in \{0, 1, 2, 3\}$

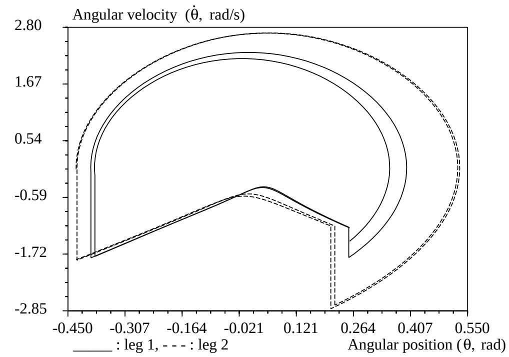

Figure 7: Phase plane limit cycle of a 4-periodic gait

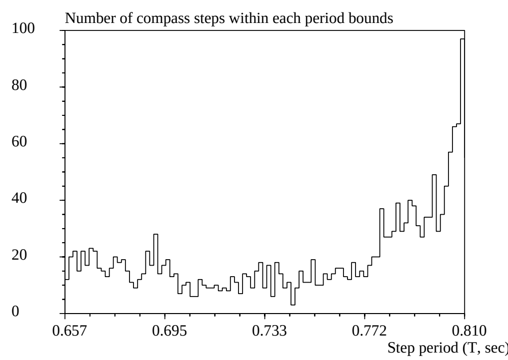

(a) chaotic passive gait: histogram of the periods of 2000 consecutive steps

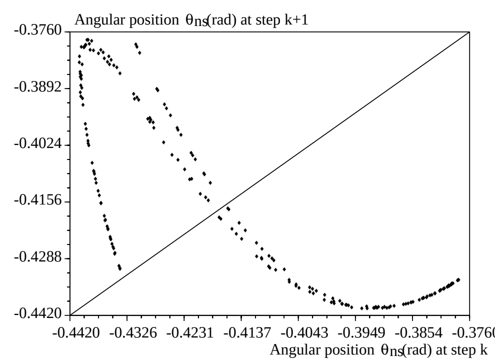

(b) First return map of θ_{ns}: chaotic gait

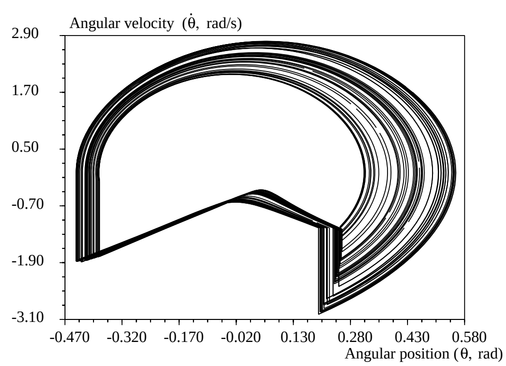

(c) Strange attractor of a chaotic steady passive gait

Figure 8: Characteristic of chaotic gait

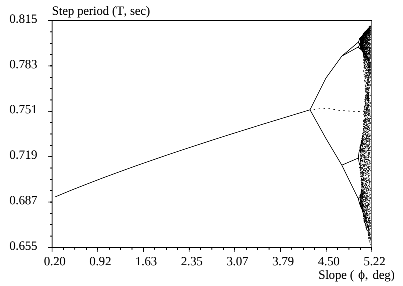

(a) Step period T as a function of ϕ

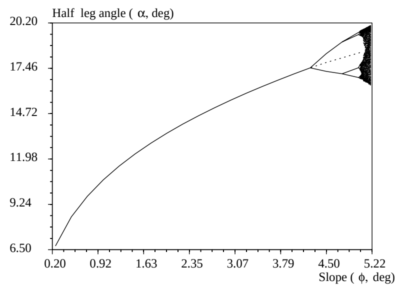

(b) Half inter-leg angle α as a function of ϕ

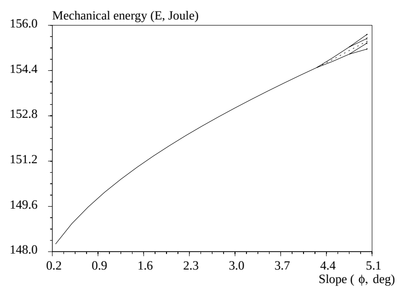

(c) Mechanical energy E as a function of ϕ

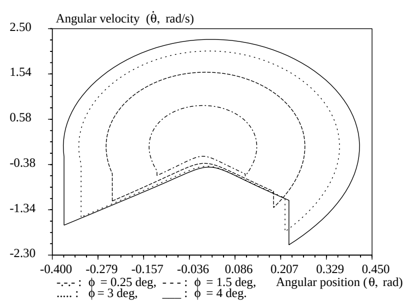

(d) Phase plane limit cycles for various values of ϕ

Figure 3: Effect of ϕ on steady gait

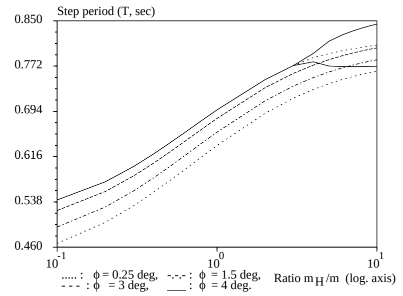

(a) Step period T as a function of μ

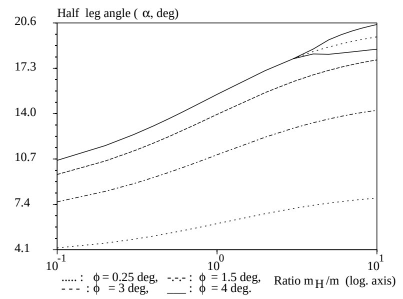

(b) Half inter-leg angle α as a function of μ

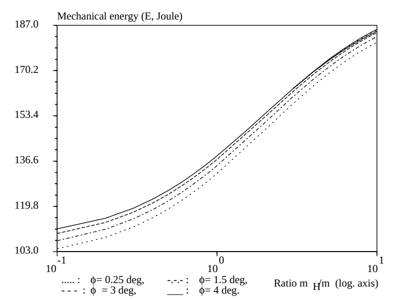

(c) Mechanical energy E as a function of μ

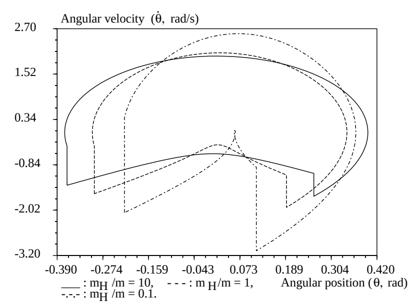

(d) Phase plane limit cycles for various values of μ

Figure 4: Effect of μ on steady gait

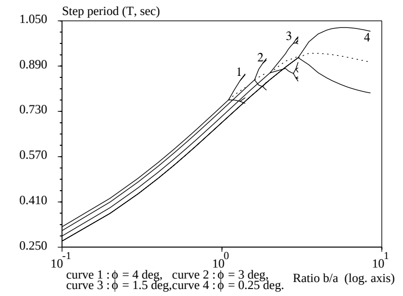

(a) Step period T as a function of β

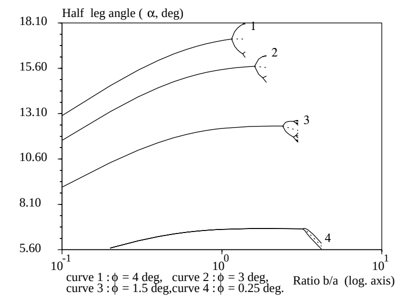

(b) Half inter-leg angle α as a function of β

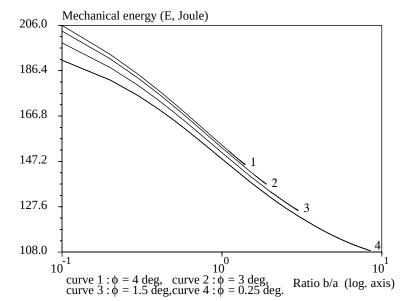

(c) Mechanical energy E as a function of β

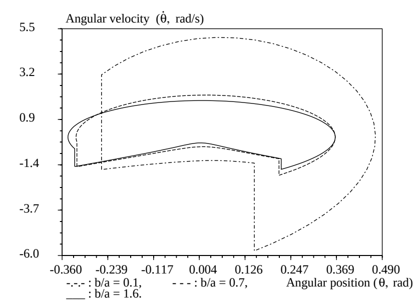

(d) Phase plane diagrams for various values of β

Figure 5: Effect of β on steady gait